https://doi.org/10.5194/tc-2023-134
Preprint. Discussion started: 11 December 2023

The Cryosphere Discussions
Open Access
EGU

Dynamic and Thermodynamic Processes Related to Sea-Ice Surface Melt Advance in the Laptev Sea and East Siberian Sea

Hongjie LIANG, [1] Wen ZHOU [1,2]

[1] *Department of Atmospheric and Oceanic Sciences & Institute of Atmospheric Sciences, Fudan University, Shanghai, China*

[2] *Center for Polar Ice & Snow and Climate Change Research, Polar Research Institute of China, Shanghai, China*

Correspondence to: Wen Zhou (wen_zhou@fudan.edu.cn)

https://doi.org/10.5194/tc-2023-134
Preprint. Discussion started: 11 December 2023

ABSTRACT

Arctic summer sea ice has shrunk considerably in recent decades. This study investigates sea-ice surface melt onset in springtime in the Laptev Sea and East Siberian Sea, which are key seas along the Northeast Passage. Melt Advance, which is defined as the areal percentage of a sea that has experienced sea-ice surface melting before the end of May, is used instead of region-mean melt onset. Four representative scenarios of Melt Advance in the region are identified. Each scenario is driven by a distinct circulation in the lower troposphere in May, which regulates sea ice dynamics and air mass transport, further influencing surface energy balance and Melt Advance. In general, concurrent with faster Melt Advance are warm and wet atmosphere, reduced sea ice cover, and surface energy gains in spring. Melt Advance, as well as sea ice cover in May, is significantly correlated with summer sea ice over. This study implicates the interannual flexibility of spring circulation in the lower troposphere and the significance of seasonal evolution in the Arctic.

1. Introduction

Since the 1970s, satellites have enabled global detection of the Earth. Arctic summer sea ice extent is found to have decreased dramatically in the past four decades (Petty et al., 2020; Stroeve & Notz, 2018), which is a prominent indicator of global warming. In fact, the Arctic has a faster warming trend than elsewhere on the planet, especially in the lower troposphere during the cold season. This phenomenon, called Arctic Amplification, results from reduced sea ice cover and enhanced oceanic energy release toward the atmosphere (Cohen et al., 2014; Serreze et al., 2009). Some research has indicated that the mid-latitudes may frequently experience severe winters due to the Arctic Amplification which reduces the meridional temperature gradient and in turn amplifies the planetary Rossby wave and makes it more stationary (Francis & Vavrus, 2015). In the Arctic, positive ice-albedo feedback is active in the melt season (Budyko,

https://doi.org/10.5194/tc-2023-134
Preprint. Discussion started: 11 December 2023

1969; Kashiwase et al., 2017; Sellers, 1969): after sea ice begins to melt in spring, surface albedo decreases substantially, which favors more solar radiation absorption and promotes further sea ice melting. Based on this notion, some studies have tried to predict Arctic summer sea ice cover by sea-ice surface Melt Onset (MO) in spring, i.e., the date when the sea ice surface begins to form liquid water (Petty et al., 2017; Wang et al., 2011). Currently, satellite remote sensing helps us construct the pan-Arctic sea ice MO, which is not possible with only in-situ field observations. For sea ice lateral and bottom melting, satellites are less useful and buoys are widely employed (Lei et al., 2022).

Many studies have touched on sea ice MO in springtime (Bliss & Anderson, 2014; Crawford et al., 2018; Drobot & Anderson, 2001; Horvath et al., 2021). Generally, sea ice MO is becoming earlier in most parts of the Arctic, which is consistent with the Arctic warming trend. Another notable feature of MO is its regionality. For example, the Barents Sea, Kara Sea, Laptev Sea, and East Siberian Sea are around the same latitudes along the Siberian coast, but the MO trends were -7.1, -5.2, -2.8, and -1.8 days per decade from 1979 to 2013, respectively (Stroeve et al., 2014). Liang and Su (2021) investigated the interannual early/late relationship of MO between the Laptev Sea and East Siberian Sea, which is related to the large-scale atmospheric pattern of the Barents Oscillation (Skeie, 2000). Locally, synoptic processes are regarded as responsible for interannual variability. Mortin et al. (2016) argued that sea ice MO is generally associated with higher surface air temperature (SAT), total-column water vapor (TWV), and cloud cover, which promotes downward longwave radiation.

Focusing on the Laptev Sea and East Siberian Sea, which usually have the heaviest ice block in the Northeast Passage, this study aims to demonstrate the springtime processes related to different MO scenarios and explore the linkage between springtime MO and summertime sea ice coverage.

https://doi.org/10.5194/tc-2023-134
Preprint. Discussion started: 11 December 2023

2. Data and Methods

Sea ice Melt Onset (MO) is the date when the sea ice surface begins to melt in spring, which is retrieved from satellite passive microwave signals (Markus et al., 2009). Liquid water has greater emissivity than ice/snow, so surface melting invokes changes in passive microwave signals. The dataset is distributed by the National Aeronautics and Space Administration (NASA) Cryospheric Sciences Research Portal. We use the yearly MO from 1979 to 2018, with a spatial resolution of ~25 km. Following the method in Liang and Su (2021), we fill in the missing MO values based on surface air temperature (SAT) datasets from the International Arctic Buoy Programme/Polar Exchange at the Sea Surface (IABP/POLES) for 1979-2004 and the Atmospheric InfraRed Sounder (AIRS) for 2005-2018.

The sea ice concentration (SIC) dataset, called Ocean and Sea Ice Satellite Application Facility (OSI SAF), is from the European Organisation for the Exploitation of Meteorological Satellites (EUMETSAT) (Lavergne et al., 2019). We use the monthly SIC from 1979 to 2018, with a resolution of 25 km.

The atmospheric variables and surface energy fluxes are from the ERA5 reanalysis by the European Centre for Medium-Range Weather Forecasts (ECMWF) (Hersbach et al., 2020), which replaces the ERA-Interim reanalysis that ceased production in 2019. The variables used in this study are monthly downward longwave radiation (DLR), net longwave radiation (NLR), downward shortwave radiation (DSR), net shortwave radiation (NSR), surface latent heat flux (SLHF), surface sensible heat flux (SSHF), total-column water vapor (TWV), and SAT and wind fields at the 850-hPa level, from 1979 to 2018. The spatial resolution of ERA5 used in this study is 0.25°×0.25°, less than 30 km in the region of the Laptev Sea and East Siberian Sea.

3. Results

3.1 Distinct Melt Advance Scenarios in the Laptev Sea and East Siberian Sea

https://doi.org/10.5194/tc-2023-134
Preprint. Discussion started: 11 December 2023

The Laptev Sea (LS) and East Siberian Sea (ESS) are marginal seas of the Arctic Ocean, north of Siberia along the Northeast Passage (Fig. S1). The longitude-latitude ranges are around 70°N-80°N and 100°E-180°, covering 0.66 and 1.14 million km^2 for the LS and ESS, respectively. These two seas are among the regions where sea ice decline in September during the past four decades has been the most prominent, and they are key regions for safe transportation across the Northeast Passage. Meanwhile, sea-ice surface Melt Onset (MO) in spring generally tends to be earlier. In spring, sea ice almost completely covers these two seas, while in summer, sea ice substantially retreats off the coast. Sea ice first begins to melt at the surface in spring when solar radiation increases and the atmosphere warms. On average, the sea ice surface begins to melt during May and June (Fig. 1a). Naturally, sea ice melting advances northward. Interannually, MO is expected to change within one month (Fig. 1b). In order to demonstrate the progress of MO in different years, melt advance (MA) is defined by calculating the areal percentage of an individual sea that has experienced MO at the end of May (see magenta contour line in Fig. 1a). In this way, we can detect whether sea-ice surface melting advances slowly or quickly in a specific year, as well as the spatial patterns. For the seasonal prediction of summer sea ice, this metric is date-dependent and useful, unlike the region-mean MO, which necessitates waiting for complete melting throughout the whole sea.

Figure 1c shows the time series of MA for the LS and ESS during 1979-2018. The variability is large, ranging from near zero to 100%. This implies changeable spring conditions on the interannual scale. On average, MA is around 40% for each sea, meaning that ~40% of the sea area has experienced sea-ice surface melting at the end of May. In the context of global warming, MA has an increasing tendency in both seas although this tendency is not quite significant (less than 6% per decade). This indicates that we sometimes need to pay more attention to the interannual variability than to the long-term linear tendency. We can also notice that relatively slow MA in the 1980s contributes considerably to the positive tendency.

https://doi.org/10.5194/tc-2023-134
Preprint. Discussion started: 11 December 2023

The Cryosphere
Discussions
Open Access

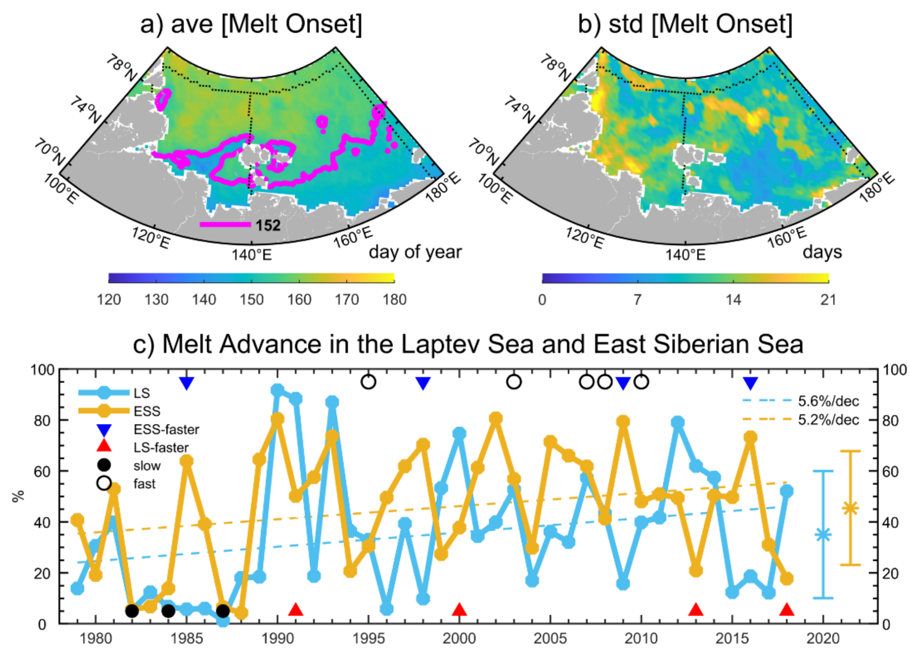

Fig. 1. (a, b) Climatology and standard deviation of sea ice Melt Onset, and (c) Melt Advance time series in the Laptev Sea and East Siberian Sea, 1979-2018. The magenta lines in panel (a) are contours of 152 (day of year), representing the end of May. The areal percentage of sea ice Melt Onset earlier than 152 (day of year) is defined as Melt Advance. In panel (c), only the trend of Melt Advance in the ESS is statistically significant at the 90% confidence level. The average and standard deviation of the Melt Advance in the LS and ESS are 35%±25% and 45%±22%, respectively. Four categories of sample years are marked (see Table 1).

Another feature is related to the relationship of MA between the LS and ESS. In some years, MA in both the LS and ESS is slow, as in the 1980s; in other years, MA in both seas may be fast; and in other years, MA can be substantially different in the two seas. Thus, four categories of sample years are selected for further composite analysis (Table 1 and markers in Fig. 1c; MA difference between the LS and ESS is shown in Fig. S2), which represent four basic scenarios of MA in this region. Specifically, years with significantly faster MA in the ESS than in the LS (δ>48%) are grouped as the ESS-faster-scenario, while years with significantly faster MA in the LS than in the ESS (δ>33%) are classified as the LS-faster-scenario. The slow-scenario includes years

https://doi.org/10.5194/tc-2023-134
Preprint. Discussion started: 11 December 2023

when MA in both seas is slow (below 20%), while the fast-scenario consists of years when MA in both seas is relatively fast (between 30% and 60% at the same time). So, two pairs of contrasting categories are formed (ESS-faster-scenario vs. LS-faster-scenario, slow-scenario vs. fast-scenario). Note that to some extent the latter two scenarios represent the contrast between the 1980s and subsequent decades. Such categorization reflects the large variability of MA in spring from the interannual perspective.

Category	Years	Description
ESS-faster-scenario	1985, 1998, 2009, 2016	significantly faster Melt Advance (δ>48%) in the ESS than in the LS
LS-faster-scenario	1991, 2000, 2013, 2018	significantly faster Melt Advance (δ>33%) in the LS than in the ESS
slow-scenario	1982, 1984, 1987	similar but slow Melt Advance (δ<8%, but below 20%)
fast-scenario	1995, 2003, 2007, 2008, 2010	similar but fast Melt Advance (δ<9%, but between 30% and 60%)

Table 1 List of years under different scenarios of Melt Advance.
Note: Practically, the ESS-faster-scenario and LS-faster-scenario are selected based on one standard deviation of the difference in Melt Advance between the Laptev Sea and East Siberian Sea. The slow-scenario and fast-scenario include years when Melt Advance in the two seas is quite close. All years listed here are marked in Fig. 1c.

Composite results show that the ESS-faster-scenario has substantially earlier MO, i.e., faster MA in the ESS than in the LS, while the LS-faster-scenario has a somewhat opposite signal (indicated by the magenta line in Fig. 2). For the slow-scenario, little area in either sea has experienced MO until the end of May, indicating slow MA; for the fast-scenario, nearly half of both seas has begun to experience sea-ice surface melting, indicating fast MA at almost the same pace. From the surface energy balance (SEB) in May, we find consistent patterns. With the zero lines of SEB as a reference, the ESS-faster-scenario has relatively more positive SEB in the ESS than in the LS, while the opposite is true for the LS-faster-scenario. For the slow-scenario, SEB is negative over most of the two seas, while for the fast-scenario, SEB is positive in both

https://doi.org/10.5194/tc-2023-134
Preprint. Discussion started: 11 December 2023

seas. This fits well with common sense. Although MA-related albedo changes may amplify the SEB signals in a two-way interaction, it is fair to say that SEB in May drives different patterns of MA (see individual years in Fig. S3).

In the next section, we investigate systematic processes under different MA scenarios that involve the atmosphere, sea ice, and surface fluxes. Note that the four components of SEB include longwave radiation, shortwave radiation, surface latent heat flux (SLHF), and surface sensible heat flux (SSHF).

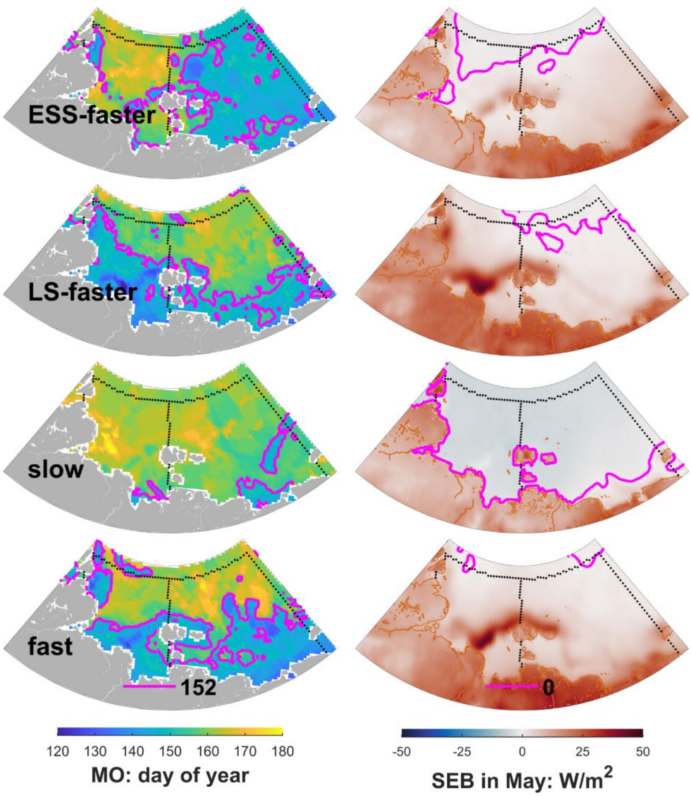

Fig. 2. Composites of MO and surface energy balance (SEB) in May for the four scenarios. The left column shows the MO patterns marked by magenta contour lines with the value of 152 (day of year) which represents the end of May. The right column is the SEB in May, with magenta contour lines of zero. Black dots denote the boundaries of the LS and ESS.

https://doi.org/10.5194/tc-2023-134
Preprint. Discussion started: 11 December 2023

3.2 Dynamic and Thermodynamic Processes under Different Melt Advance Scenarios

Climatologically, SEB is basically positive (~5 W/m^2) across the two seas in May (see first row in Fig. S4). Among the components, it is positive net shortwave radiation (NSR) that compensates for losses from net longwave radiation (NLR), SLHF, and SSHF. This implies that on average the atmosphere receives energy from the surface through the latter three components in May. SAT is around -6°C, while sea ice almost fully covers the ocean (~90%) (see first row in Fig. 3). In the lower troposphere (850 hPa), southeasterlies blow across the region, which to some extent explains the existence of polynyas in the middle LS, i.e., regions where sea ice concentration is below 75%. Note that Fig. 3 shows only selected vital variables; other relevant factors can be found in Fig. S4-S7.

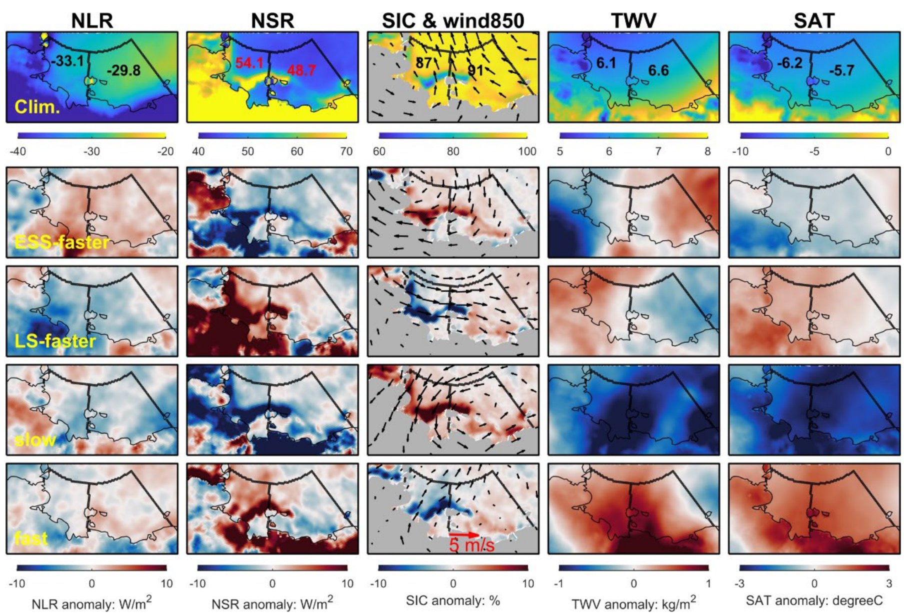

Fig. 3. Climatology (first row) and composite anomalies for the four scenarios (lower four rows) of relevant atmospheric and sea ice variables in May: NLR, NSR, SIC, winds at 850 hPa, TWV, and SAT. Numbers within the LS and ESS are the region-mean values, respectively.

In the ESS-faster-scenario (see second row in Fig. 3 and blue bars in Fig. 4),

https://doi.org/10.5194/tc-2023-134
Preprint. Discussion started: 11 December 2023

prevailing northeasterlies in the lower troposphere push and consolidate the sea ice against the land, especially for the LS, which increases surface albedo and decreases solar radiation absorption. The northeasterlies seem to also bring slightly cool air masses to the region, and slightly moist air masses to the ESS. As a whole, the atmospheric state is close to climatology as shown by small SAT and TWV anomalies. Given that sea ice cover is more packed, longwave radiation loss from the surface to the atmosphere is reduced, which to some extent compensates for the reduced solar radiation absorption. Due to the greater reduction of solar radiation absorption in the LS, the net surface energy balance is a loss in the LS, but a gain in the ESS. In addition, sea-ice surface melting is usually preconditioned by increased water vapor in the atmosphere (Mortin et al., 2016). So, faster Melt Advance in the ESS is expected as TWV is increased in the ESS.

For the LS-faster-scenario (see third row in Fig. 3 and red bars in Fig. 4), wind fields at 850-hPa show unified westerlies over the LS and northwesterlies over the ESS, which account for the reduced sea ice cover in the LS and the slightly packed sea ice in the ESS. So, we see a substantial increase in solar radiation absorption (beyond one standard deviation) in the LS. Given that longwave radiation loss is somehow enhanced, the net surface energy balance is still a gain for the LS and a loss for the ESS. The westerlies may also contribute to positive anomalies of TWV and SAT in the LS, which promotes faster MA. It is also possible that reduced sea ice cover in the LS enables more moisture to be released from the exposed ocean.

https://doi.org/10.5194/tc-2023-134
Preprint. Discussion started: 11 December 2023

The Cryosphere Discussions
Open Access
EGU

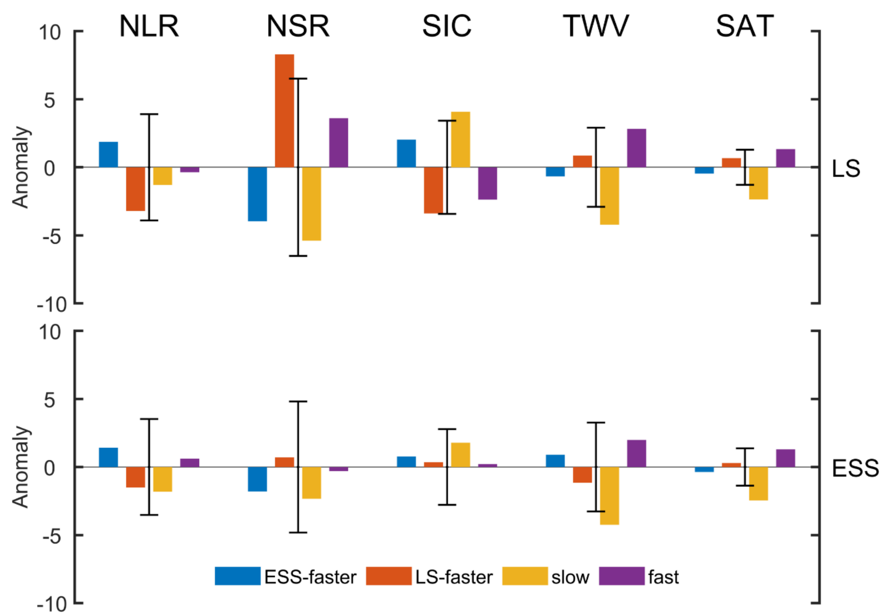

Fig. 4. Region-mean composite anomalies in the LS and ESS for the four scenarios shown in Fig. 3. The error bars denote the corresponding standard deviation for 1979-2018. The variables of NLR, NSR, SIC, TWV, and SAT have units of W/m^2, W/m^2, %, kg/m^2, and K, respectively. Here, SIC is represented by the areal percentage of sea ice cover relative to the whole sea. To facilitate viewing, TWV is scaled by a factor of 5.

For the slow-scenario, with three sample years from the 1980s (see fourth row in Fig. 3, and orange bars in Fig. 4), a cyclonic anomaly in the lower troposphere, which is centered on the ESS, pushes sea ice against the southern coast in the LS. More sea ice cover in both seas decreases solar radiation absorption. Meanwhile, this circulation also brings this region under the influence of cold and dry air masses (beyond one standard deviation), which induce a large loss of longwave radiation and SSHF from the surface. As a whole, we see unified surface energy deficits in the LS and ESS (beyond one standard deviation). Slow MA is also expected for this region.

For the fast-scenario, with sample years after the 1980s (see last row in Fig. 3, and purple bars in Fig. 4), southerlies in the lower troposphere blow mainly across the LS, which drive sea ice off the coast and in turn increase shortwave radiation absorption. At the same time, the southerlies bring warm and wet air masses to this region, which

https://doi.org/10.5194/tc-2023-134
Preprint. Discussion started: 11 December 2023

substantially reduce the SSHF loss from the surface. As a result, we see a positive net surface energy balance in this region and relatively fast MA.

The composite analysis above indicates that circulation in the lower troposphere in spring in this region can be quite changeable (see individual years in Fig. S8), which can have two effects: one is related to sea ice dynamics; the other involves moisture and warm air advection. The former produces strong regulation of NSR due to albedo changes, while the latter has everything to do with the atmospheric state, which favors sea-ice surface melting when the atmosphere is warm and wet.

Figure 5 further shows the statistical correlation related to MA, incorporating years from 1979 to 2018. In general, we see that faster MA is accompanied by warm and wet atmosphere. The related atmospheric circulation in the lower troposphere may also drive reduced SIC and subsequent increased solar radiation absorption. In addition, previous studies have argued that on a synoptic scale, increased water vapor in the atmosphere favors stronger DLR, which promotes sea-ice surface melting. The result here suggests that on the subseasonal scale longwave radiation has little connection with MA (see first column in Fig. 5). Other relevant variables can be found in Fig. S9.

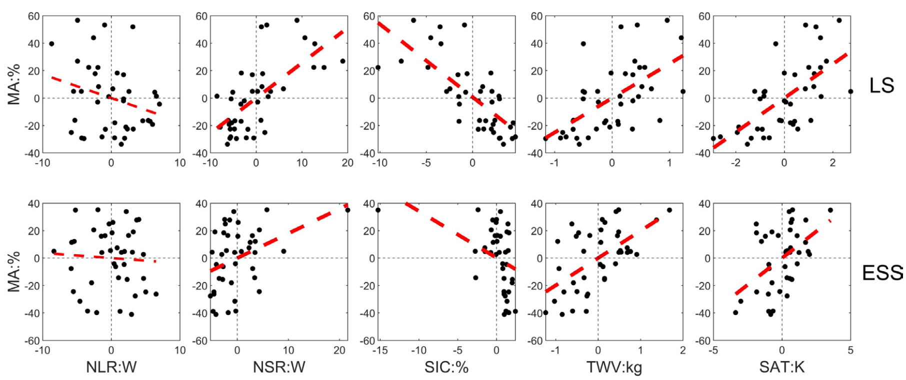

Fig. 5. Scatter plots for 1979-2018 between the MA anomaly and region-mean anomalies of factors shown in Figs. 3 and 4. Thick dashed red lines denote linear fits above the 95% confidence level.

https://doi.org/10.5194/tc-2023-134
Preprint. Discussion started: 11 December 2023

4. Discussion

In this study, sampling for different scenarios of sea ice Melt Advance is based on the Melt Onset dataset, which is a satellite observation product. To our knowledge, ERA5 to some extent incorporates the sea ice concentration dataset of OSI SAF, but not the Melt Onset dataset (Hersbach et al., 2020). ERA5 atmospheric reanalysis and different Melt Advance patterns can be seen as independent sources of information and their consistency should provide more confidence.

In fact, the concept of Melt Advance can be used for the whole Arctic, and can describe how sea-ice surface melting advances in spring. As mentioned above, Melt Advance can also be used as relatively independent information with reference to an atmospheric reanalysis dataset. In previous work, three modes of Melt Onset in the LS and ESS are identified by EOF decomposition (Liang and Zhou, 2023, in press), and to some extent correspond to the different Melt Advance scenarios in this work.

To what extent do different sea-ice surface melting scenarios in spring have implications for sea ice cover in summer? Could we gain seasonal prediction skill based on detection of sea-ice surface melting in spring? A simple way to address this is to put aside the processes linking spring and summer and directly investigate the statistical relationship between sea-ice surface melting scenarios in spring and sea ice states in summer. Figure 6 shows that in both the LS and ESS, Melt Advance in spring is significantly correlated with sea ice cover in September, which is consistent with previous studies utilizing Melt Onset as a predictor of summer sea ice (Petty et al., 2017; Wang et al., 2011). However, it has no stronger prediction skill than SIC in May. Beyond this, for the prediction of summer sea ice cover, the seasonal evolution from spring to summer is still a challenge as it is not fully understood. Processes during the melting season may strongly disturb the signal from the Melt Advance (Fig. S10). More study of seasonal evolution in the Arctic is needed in the future.

https://doi.org/10.5194/tc-2023-134
Preprint. Discussion started: 11 December 2023

The Cryosphere
Discussions
Open Access
EGU

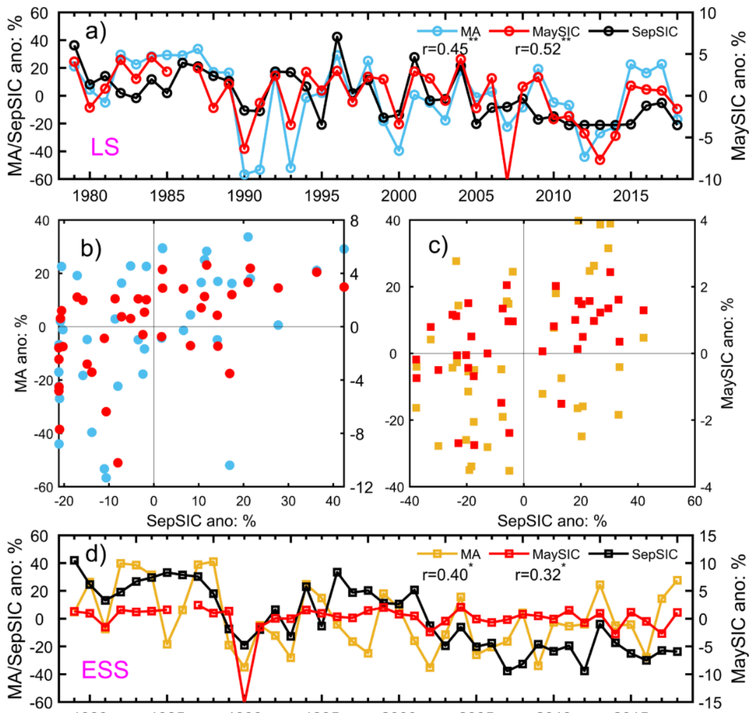

Fig. 6. Sea-ice surface Melt Advance, SIC in May and September sea ice cover in the Laptev Sea (subplot a and b) and East Siberian Sea (subplot c and d), 1979-2018. September sea ice cover is denoted by the areal percentage of sea ice cover relative to the whole sea. To facilitate viewing, Melt Advance is timed by -1. Correlation coefficients with double asterisks denote 99% confidence, while those with a single asterisk denote 90% confidence.

5. Conclusions

In this study, the metric of Melt Advance (MA) is used to measure sea-ice surface melting instead of region-mean Melt Onset. MA is defined as the areal percentage of a sea in which the sea ice surface has begun to melt at the end of May, in this case the Laptev Sea (LS) and East Siberian Sea (ESS). This metric has the potential to help seasonally predict summer sea ice, as this can be a temporally changing variable. Melt Advance is also a potential metric for the whole Arctic.

Four representative scenarios of Melt Advance in the LS and ESS are identified: the

https://doi.org/10.5194/tc-2023-134
Preprint. Discussion started: 11 December 2023

ESS-faster-scenario, LS-faster-scenario, slow-scenario, and fast-scenario. Composite analyses reveal that the dominant driver is circulation in the lower troposphere, which regulates sea ice dynamics as well as air mass advection. The surface energy balance and sea ice Melt Advance are then influenced. The main conclusions are demonstrated in the schematic in Fig. 7.

Although sea ice Melt Advance as well as sea ice cover in May are both statistically correlated with sea ice cover in September, seasonal evolution can to a large extent disturb this linkage. This study suggests a need to further investigate the changeable spring circulation in the lower troposphere and seasonal evolution in the Arctic.

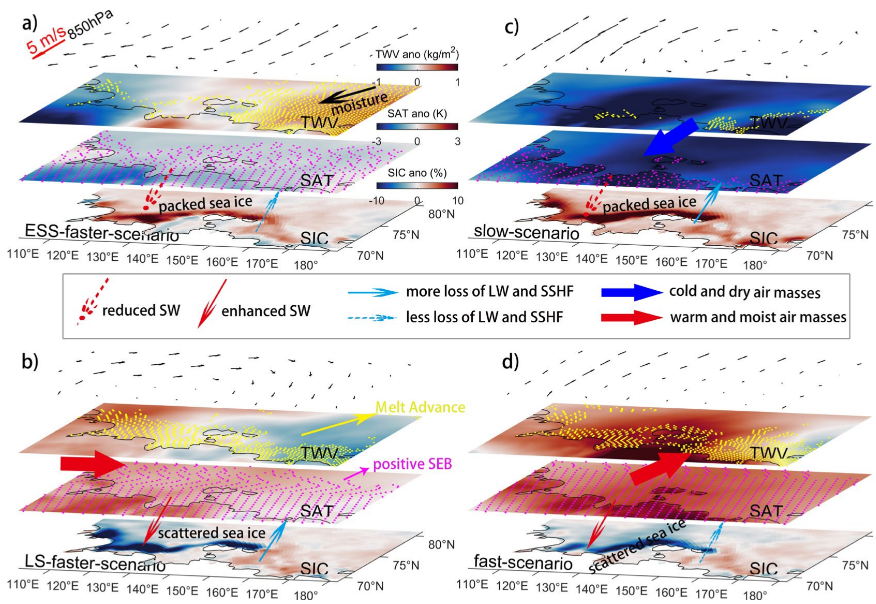

Fig. 7. Schematic processes under the four scenarios of sea ice Melt Advance in the LS and ESS

https://doi.org/10.5194/tc-2023-134
Preprint. Discussion started: 11 December 2023

Data Availability Statement.

The sea ice MO dataset is from NASA's Cryospheric Sciences Research Portal (https://earth.gsfc.nasa.gov/cryo/data/arctic-sea-ice-melt). SAT of IABP/POLES can be accessed at https://arcticdata.io/catalog/view/doi:10.18739/A2J598, and SAT of AIRS at https://disc.gsfc.nasa.gov/datasets/AIRS3STD_006/summary. The SIC dataset of OSI SAF was downloaded from the websites below: ftp://osisaf.met.no/reprocessed/ice/conc/v2p0/ and ftp://osisaf.met.no/reprocessed/ice/conc-cont-reproc/v2p0/.

The ERA5 reanalysis dataset was retrieved at https://cds.climate.copernicus.eu/cdsapp#!/search?type=dataset&keywords=((%20%22Product%20type:%20Reanalysis%22%20). In this study, we used ERA5 monthly averaged data at single levels and pressure levels.

Author Contribution

Hongjie Liang [Formal analysis; Writing original draft]. Wen Zhou [Funding acquisition; Supervision].

Competing interests

The authors declare that they have no conflict of interest.

Acknowledgments.

This work was supported by the National Natural Science Foundation of China (Grant No. 42288101, 42120104001).

REFERENCES

Bliss, A., & Anderson, M. (2014). Snowmelt onset over Arctic sea ice from passive microwave satellite data: 1979–2012. *The Cryosphere*, *8*(6), 2089-2100. https://doi.org/10.5194/tc-8-2089-2014

Budyko, M. I. (1969). The effect of solar radiation variations on the climate of the Earth. *Tellus*, *21*(5), 611-619. https://doi.org/10.1111/j.2153-3490.1969.tb00466.x

Cohen, J., Screen, J. A., Furtado, J. C., Barlow, M., Whittleston, D., Coumou, D., . . .

https://doi.org/10.5194/tc-2023-134
Preprint. Discussion started: 11 December 2023

Jones, J. (2014). Recent Arctic amplification and extreme mid-latitude weather. *Nature Geoscience*, *7*(9), 627-637. https://doi.org/10.1038/ngeo2234

Crawford, A. D., Horvath, S., Stroeve, J., Balaji, R., & Serreze, M. C. (2018). Modulation of Sea Ice Melt Onset and Retreat in the Laptev Sea by the Timing of Snow Retreat in the West Siberian Plain. *Journal of Geophysical Research: Atmospheres*, *123*(16), 8691-8707. https://doi.org/10.1029/2018jd028697

Drobot, S. D., & Anderson, M. R. (2001). An improved method for determining snowmelt onset dates over Arctic sea ice using scanning multichannel microwave radiometer and Special Sensor Microwave/Imager data. *Journal of Geophysical Research: Atmospheres*, *106*(D20), 24033-24049. https://doi.org/10.1029/2000JD000171

Francis, J. A., & Vavrus, S. J. (2015). Evidence for a wavier jet stream in response to rapid Arctic warming. *Environmental Research Letters*, *10*(1). https://doi.org/10.1088/1748-9326/10/1/014005

Hersbach, H., Bell, B., Berrisford, P., Hirahara, S., Horányi, A., Muñoz‐Sabater, J., . . . Thépaut, J. N. (2020). The ERA5 global reanalysis. *Quarterly Journal of the Royal Meteorological Society*, *146*(730), 1999-2049. https://doi.org/10.1002/qj.3803

Horvath, S., Stroeve, J., Rajagopalan, B., & Jahn, A. (2021). Arctic sea ice melt onset favored by an atmospheric pressure pattern reminiscent of the North American-Eurasian Arctic pattern. *Climate Dynamics*, *57*(7-8), 1771-1787. https://doi.org/10.1007/s00382-021-05776-y

Kashiwase, H., Ohshima, K. I., Nihashi, S., & Eicken, H. (2017). Evidence for ice-ocean albedo feedback in the Arctic Ocean shifting to a seasonal ice zone. *Sci Rep*, *7*(1), 8170. https://doi.org/10.1038/s41598-017-08467-z

Lavergne, T., Sørensen, A. M., Kern, S., Tonboe, R., Notz, D., Aaboe, S., . . . Pedersen, L. T. (2019). Version 2 of the EUMETSAT OSI SAF and ESA CCI sea-ice concentration climate data records. *The Cryosphere*, *13*(1), 49-78. https://doi.org/10.5194/tc-13-49-2019

Lei, R., Cheng, B., Hoppmann, M., Zhang, F., Zuo, G., Hutchings, J. K., . . . Nicolaus, M. (2022). Seasonality and timing of sea ice mass balance and heat fluxes in the Arctic transpolar drift during 2019–2020. *Elementa: Science of the Anthropocene*, *10*(1). https://doi.org/10.1525/elementa.2021.000089

Liang, H., & Su, J. (2021). Variability in Sea Ice Melt Onset in the Arctic Northeast Passage: Seesaw of the Laptev Sea and the East Siberian Sea. *Journal of Geophysical Research: Oceans*, *126*(10), e2020JC016985. https://doi.org/10.1029/2020JC016985

Markus, T., Stroeve, J. C., & Miller, J. (2009). Recent changes in Arctic sea ice melt onset, freezeup, and melt season length. *Journal of Geophysical Research (Oceans)*, *114*, C12024. https://doi.org/10.1029/2009jc005436

Mortin, J., Svensson, G., Graversen, R. G., Kapsch, M.-L., Stroeve, J. C., & Boisvert, L. N. (2016). Melt onset over Arctic sea ice controlled by atmospheric

https://doi.org/10.5194/tc-2023-134
Preprint. Discussion started: 11 December 2023

moisture transport. *Geophysical Research Letters*, *43*(12), 6636-6642. https://doi.org/10.1002/2016GL069330

Petty, A. A., Kurtz, N. T., Kwok, R., Markus, T., & Neumann, T. A. (2020). Winter Arctic Sea Ice Thickness From ICESat‐2 Freeboards. *Journal of Geophysical Research: Oceans*, *125*(5). https://doi.org/10.1029/2019jc015764

Petty, A. A., Schröder, D., Stroeve, J. C., Markus, T., Miller, J., Kurtz, N. T., . . . Flocco, D. (2017). Skillful spring forecasts of September Arctic sea ice extent using passive microwave sea ice observations. *Earth's Future*, *5*(2), 254-263. https://doi.org/10.1002/2016ef000495

Sellers, W. D. (1969). A Global Climatic Model Based on the Energy Balance of the Earth-Atmosphere System. *Journal of Applied Meteorology and Climatology*, *8*(3), 392-400. https://doi.org/10.1175/1520-0450(1969)008<0392:agcmbo>2.0.co;2

Serreze, M. C., Barrett, A. P., Stroeve, J. C., Kindig, D. N., & Holland, M. M. (2009). The emergence of surface-based Arctic amplification. *The Cryosphere*, *3*(1), 11-19. https://doi.org/10.5194/tc-3-11-2009

Skeie, P. (2000). Meridional flow variability over the Nordic Seas in the Arctic oscillation framework. *Geophysical Research Letters*, *27*(16), 2569-2572. https://doi.org/10.1029/2000gl011529

Stroeve, J., & Notz, D. (2018). Changing state of Arctic sea ice across all seasons. *Environmental Research Letters*, *13*(10), 103001. https://doi.org/10.1088/1748-9326/aade56

Stroeve, J. C., Markus, T., Boisvert, L., Miller, J., & Barrett, A. (2014). Changes in Arctic melt season and implications for sea ice loss. *Geophysical Research Letters*, *41*(4), 1216-1225. https://doi.org/10.1002/2013gl058951

Wang, L., Wolken, G. J., Sharp, M. J., Howell, S. E. L., Derksen, C., Brown, R. D., . . . Cole, J. (2011). Integrated pan-Arctic melt onset detection from satellite active and passive microwave measurements, 2000-2009. *Journal of Geophysical Research: Atmospheres*, *116*(D22). https://doi.org/10.1029/2011jd016256